Cellular and Molecular Life Sciences (2018) 75:2027–2044
https://doi.org/10.1007/s00018-017-2719-2

ORIGINAL ARTICLE

Sorting nexin 3 mutation impairs development and neuronal function in *Caenorhabditis elegans*

Neide Vieira[1,2] · Carlos Bessa[1,2] · Ana J. Rodrigues[1,2] · Paulo Marques[1,2] · Fung-Yi Chan[3,4] · Ana Xavier de Carvalho[3,4] · Margarida Correia-Neves[1,2] · Nuno Sousa[1,2]

Received: 17 August 2017 / Revised: 27 October 2017 / Accepted: 22 November 2017 / Published online: 1 December 2017

Abstract

The sorting nexins family of proteins (SNXs) plays pleiotropic functions in protein trafficking and intracellular signaling and has been associated with several disorders, namely Alzheimer's disease and Down's syndrome. Despite the growing association of SNXs with neurodegeneration, not much is known about their function in the nervous system. The aim of this work was to use the nematode *Caenorhabditis elegans* that encodes in its genome eight SNXs orthologs, to dissect the role of distinct SNXs, particularly in the nervous system. By screening the *C. elegans* SNXs deletion mutants for morphological, developmental and behavioral alterations, we show here that *snx-3* gene mutation leads to an array of developmental defects, such as delayed hatching, decreased brood size and life span and reduced body length. Additionally, Δ*snx-3* worms present increased susceptibility to osmotic, thermo and oxidative stress and distinct behavioral deficits, namely, a chemotaxis defect which is independent of the described *snx-3* role in Wnt secretion. Δ*snx-3* animals also display abnormal GABAergic neuronal architecture and wiring and altered AIY interneuron structure. Pan-neuronal expression of *C. elegans snx-3* cDNA in the Δ*snx-3* mutant is able to rescue its locomotion defects, as well as its chemotaxis toward isoamyl alcohol. Altogether, the present work provides the first in vivo evidence of the SNX-3 role in the nervous system.

Keywords Behavior · Neuronal defects · Impaired development · Nervous system · Sorting nexins

Introduction

Recently, sorting nexins (SNXs) emerged as a novel family of highly conserved proteins that facilitate protein trafficking and cell signaling [1, 2]. SNXs modulate the presence/abundance of proteins at the cell surface and also their pathological accumulation/clearance. To date 33 mammalian SNXs have been identified and the hallmark of the family is a modestly conserved phosphoinositol-binding PX domain [1]. Reports linking SNXs and endocytic events underlying diseases of the central nervous system (CNS) are growing in number [2]. Specifically, abnormal SNXs expression has been shown to cause a rare cerebellar ataxia and intellectual disability syndrome [3], to be associated with Alzheimer's disease (AD) [4–7], with Down's syndrome (DS) [8], among others. Interestingly, synaptic and cognitive deficits have been rescued by modulating SNXs expression levels [8]. SNXs have also been linked to schizophrenia [9, 10]. Particularly, SNX19 elevated expression is associated with the risk of developing schizophrenia, and single-nucleotide polymorphisms (SNPs) that contribute to the onset of the disease has been identified [9, 11]. Overall, despite the solid evidence that alterations in SNXs expression levels contribute to neurodegeneration and cognitive impairment, their role in the CNS remains largely unknown.

Caenorhabditis elegans has been widely used as a multicellular model organism to study physiological functions

Margarida Correia-Neves and Nuno Sousa share senior authorship.

✉ Nuno Sousa
njcsousa@med.uminho.pt

1 School of Medicine, Life and Health Sciences Research Institute (ICVS), University of Minho, Campus Gualtar, 4710-057 Braga, Portugal

2 ICVS/3B's-PT Government Associate Laboratory, Braga/Guimarães, Portugal

3 i3S-Instituto de Investigação e Inovação em Saúde, Universidade do Porto, Porto, Portugal

4 Instituto de Biologia Molecular e Celular-IBMC, Porto, Portugal

and malfunctions of the nervous system due to its well-described neuronal lineage, interconnectivity and amenability to genetic manipulation [12]. *C. elegans* encodes in its genome eight predicted SNX homologs, from which three members (SNX-1, SNX-6 and SNX-9) are PX-BAR domain containing SNXs, being expected to play a role in protein dimerization, membrane curvature sensing and in membrane tubulation; one member (SNX-3) is of the PX-only subfamily that plays pleiotropic functions; two members (SNX-13 and SNX-14) of the PXA-RGS-PX-PXC subfamily, which are expected to modulate G-protein coupled receptor signaling; and two members (SNX-17 and SNX-27) of the PX-FERM subfamily, notorious for their scaffolding and trafficking functions [2]. *C. elegans* SNX-s' expression pattern and function are poorly described; however, there are strong indications that several of them are associated with the retromer complex [13].

The retromer complex is a heterotrimeric complex conserved across all eukaryotes, which is composed by the VPS26 (vacuolar protein sorting-associated protein 26), VPS29 and VPS35 proteins. These VPS proteins engage in cargo loading into membrane tubules coated by the PX-BAR proteins: SNX1, SNX2, SNX5 and SNX6, aiding on cargo retrieval from the endo-lysosomal pathway [13, 14]. This retromer-dependent recycling is crucial for several processes, namely to the establishment of Wnt signaling gradients, glutamate receptor trafficking and amyloid percursor protein (APP) trafficking in the brain of mammals [8, 15–17]. Hence, it is not surprising that the dysfunction of the retromer-mediated endosomal protein sorting has been shown to occur in distinct pathologies of the nervous system [18]. To date, *C. elegans* SNX-1, SNX-3 and SNX-6 have been reported to interact with this complex [15, 19, 20], in a manner similar to their mammalian homologs [1, 21]. Particularly, *C. elegans* SNX-1 has been reported to interact with RME-8, a J-DNA protein [22, 23], and both Δ*snx-1* and Δ*rme-8* missort Wntless/MIG-14 (Wls), impacting on the polarity of mechanosensory neurons, and hence on Wnt signaling [23]. SNX-3 has also been shown to play a critical role in Wnt signaling (EGL-20), and in Wls recycling, both in mammals and in the worm, through its interaction with the retromer complex [15]. Recently, SNX-3 and VPS-35 have also been found to regulate the correct trafficking of the retrograde cargoes type I TGF- β receptor (SMA-6), and TGN-38, in the worm [24, 25]. SNX-1, SNX-6 and SNX-9 have additionally been associated with the PI3P-mediated degradation of apoptotic cells [26, 27]. Currently, SNX-13, SNX-14, SNX-17 and SNX-27 functions remain to be characterized. Overall there are strong evidences that some of *C. elegans* SNXs orthologs play important roles on cargo recycling through the retromer complex, by interacting with distinct regulatory proteins that dictate the retrieval of different cargoes from the endo-lysosomal fate and that this is conserved in mammals [28, 29]. Nevertheless, the biological function of *C. elegans* SNXs orthologs and their relevance to the nervous system has not been addressed.

In this work, we describe for the first time a phenotypical characterization of all the viable *C. elegans* SNXs deletion mutants. Overall, despite the strong association of SNXs with retromer function, and the implications of retromer dysfunction in brain pathology, our results indicate that the disruption of SNXs, with exception to SNX-3, has no obvious impact on the worm's survival, development and in the execution of distinct behaviors. Interestingly, disrupting SNX-3 pronouncedly impacts on the worm's ability to develop and reduces its lifespan. Δ*snx-3* mutant also displays severe motor impairments, reduced stress tolerance and altered mechanosensory behaviors such as thermotaxis and chemotaxis. Accordingly, the Δ*snx-3* mutant presents marked defects in its GABAergic neuronal wiring, and also in the structure of its AIY interneuron. Interestingly, the Δ*snx-3* mutant inability to chemotract towards isoamyl alcohol occurs independently of SNX-3 reported role in Wnt signaling or retromer function. In this study, we also demonstrate that impaired behaviors of the Δ*snx-3* mutant, namely its motility and chemotaxis towards isoamyl alcohol, are rescued by transgenic neuronal expression of *C. elegans snx-3* cDNA. Overall, our results suggest that SNX-3 plays important roles in the CNS, that occur independently of its role in Wnt secretion and interaction with the retromer complex.

Materials and methods

Caenorhabditis elegans strains and general methods

Caenorhabditis elegans strains used in this work: [N2 (wild-type); Δ*snx-1/2* (*tm847*), Δ*snx-3/12* (*tm1595*), Δ*snx-5/6* (*tm3790*), Δ*snx-9/Lst-4* (*tm2423*), Δ*snx-13/25* (*tm2404*), Δ*snx-17* (*tm3779*) and Δ*snx-27* (*tm5356*)] were obtained from the National BioResource Project in Japan. *Osm-6* and *osm-9* were used as controls in the chemotaxis assays; *daf-2* (*e1370*) and *daf-16* (*mu86*) were used for lifespan assays. The mutant *vps-35* (*hu68*) was used as a general retromer mutant; *egl-20* (*n585*) as a Wnt signaling mutant; and *mig-14* (*ga62*) and *mig-14* (*mu71*) as Wls mutants (the only viable *mig-14* deletion mutants, being *mu71* weaker). EG1285 (oxIs12[Punc-47::GFP; lin-15(+)]) and OH3701 (otIs173 [F25B3.3::DsRed2 + ttx-3pB::GFP]) transgenes were used for neuronal architecture analysis. All the above strains were kindly provided by the *Caenorhabditis* Genetics Center (CGC), which is funded by NIH office of research infrastructure program (P40 OD010440). Mutant genotyping was performed by standard PCR using primers listed on Table 1. *C. elegans* strains were grown according to standard conditions [30] at 20 °C in NGM plates seeded with

Table 1 List of primers used for mutant genotyping

C. elegans gene	*C. elegans* mutant	Mutant (alleles)	Forward primer	Reverse primer
SNX1/2	*Δsnx-1*	*tm847*	ACTGCGATGAGATCAACTTG	TCTCAGTGACGTCGGTCAGT
SNX3/12	*Δsnx-3*	*tm1595*	TGGAAAAATGCGCTACACGG	TGGTGATGGGGACAAAGTAC
SNX5/6	*Δsnx-5*	*tm3790*	TCAGCACCGAACCGAGGAGA	ACCAGTTTTTCTCGAAAAGC
SNX9	*Δsnx-9*	*tm2423*	GTAGCCACTCGGAACACGGT	GGAGCCAAACTTCCGACTGA
SNX13/25	*Δsnx-13*	*tm2404*	ACATTCGGTTCAACCGGTCT	AATCAACCTGGCGGAGACTG
SNX17	*Δsnx-17*	*tm3779*	CCGGATACGAAGACACTAGT	TTGGCAACCAATGGATGTCC
SNX27	*Δsnx-27*	*tm5356*	TCGTCAATGTTTCCGGTCGA	TGCCATTGAACTCTCTTCTCCA

Table 2 List of primers used for cDNA amplification of *snx-3*

C. elegans gene	Forward primer	Reverse primer
snx-3	GGGGACAAGTTTGTACAAAAAAGCAGGCTCCATGGC ATCCGGCGCGTCG	GGGGACCACTTTGTACAAGAAAGCTGGGTCTTAAGC GGTACGAATTTTG

Escherichia coli, OP50 strain. Hermaphrodite worms were used in all tests.

Cloning procedures and transgenics creation

Total RNA was isolated from N2 wild type strain using Trizol; 2 µg of total RNA was reverse transcribed into cDNA using iScript (Biorad). *C. elegans snx-3* cDNA was amplified using Platinum Taq DNA Polymerase High Fidelity (Thermo Fisher Scientific) with primers cesnx-3_attB1 and cesnx-3_attB2 (Table 2), and was cloned into pDONR221 using Gateway BP Clonase II Enzyme (Invitrogen). *Homo sapiens Snx-3* cDNA containing vector was purchased from Dharmacon (OHS5893-202499261; pENTR221-Snx-3). The pDONR or pENTR clones were transferred into destination vectors for *C. elegans* expression using Gateway LR Clonase II Enzyme. Destination vectors pDEST-aex-3p (neuronal expression) and pDEST-eft-3p (ubiquitous expression) were a generous gift from Hidehito Kuroyanagi [31]. Final pDEST vectors were sequenced and injected in wild-type (N2) worms at 50 ng/µl, together with the marker plasmid, pCFJ90 (myo-2::mCherry) at 5 ng/µl. Fluorescent worms were isolated as individual clones, which were then crossed with *Δsnx-3* worms. Distinct transgenic strains were generated, as presented in Table 3.

Table 3 List of strains generated in this work

Name	Genotype
tm1595;SOUEx1	*tm1595;paex-3::snx-3;pmyo::mcherry*
tm1595;SOUEx2	*tm1595;paex-3::snx-3;pmyo::mcherry*

Phylogenetic studies

A phylogenetic tree was elaborated for SNXs orthologs (*H. sapiens*, *Rattus norvegicus*, *Mus musculus* and *C. elegans*). Protein sequences were obtained from NCBI and Wormbase and aligned by log-expectation using the Muscle alignment web server [32]. Neighbour-joining phylogenies were generated using Protdist and Neighbour programs from the PHYLIP package (http://evolution.genetics.washington.edu/phylip.html) and displayed using Treeview. The percentage of amino acid identity (similarity in parenthesis) of each functional domain between *C. elegans* proteins and its mammalian SNXs orthologs was assessed using EMBOSS MATCHER.

Quantitative real-time PCR analysis

Total RNA was isolated from *C. elegans* wild-type strain at different stages of development (egg, L1/L2, L3, L4 and young adult), as well as of young adult Δ*snx-s*, retromer and wnt-related mutants used in this study. RNA was isolated using Trizol and following the manufacturer's instructions (Invitrogen, USA). For cDNA synthesis 1 µg of RNA was treated with DNAse (Roche) and then converted into cDNA using the iscript kit (Biorad). The cDNA was amplified from total RNA obtained from wild-type animals collected at distinct stages of development, from three independent experiments. qRT-PCR was performed in a Biorad q-PCR CFX96 apparatus with Evagreen dye (Biorad). A melting curve analysis was also carried out to verify the specificity of amplicons. The ΔΔCt method was used to quantify the amount of mRNA level relative to that of two house keeping

genes: actin and RPB-2 [33, 34]. The list of oligonucleotides used for qRT-PCR analysis are listed on Table 4.

Morphological analysis

The length of the worms was measured during development. Worms were synchronized by bleaching and around 80–100 eggs were transferred into 60 mm plates with motility seeding and were photographed on day 1, 2, 3 and 4 post-hatching using the SXZ7 + SC30 combo (dissecting microscope and camera) at a 12.5× magnification, using the CellSens program. Morphology analysis was performed with the image processing program ImageJ and the length calculated for each strain (≥ 50 worms per strain, per day post-hatching).

Brood size analysis and *ex-utero* development

For brood size measurements 20 L4 animals, per strain, were kept at 20 °C in individual plates and allowed to lay eggs. Animals were transferred to new plates daily and total progeny counted in the first 4–5 days. For the development assay ten adult worms, per strain, were placed individually on plates with fresh bacterial lawns and allowed to lay eggs for 2 h at 20 °C. Adults were then removed and the number of eggs/worms counted on each plate at distinct time points. Day 1–2 (10–24 h) for L1 and unhatched egg calculation, and day 3 (48–60 h) for L4 calculation.

Motility and crawling speed analysis

Synchronous cultures were maintained at 20 °C and 3-, 4- and 5-day-old worms analyzed. Five animals were placed in the center of a freshly seeded plate (acclimatized at 20 °C). Animals were allowed to move freely in the plate for 1 min and animals that remained inside the 1-cm circle were scored as locomotion-defective. A total of more than 100 animals were scored in at least three independent assays per strain. The worm movement was analyzed by tracking several worms on video, and by determining the average crawling speed. The videos were recorded with an Olympus SC30 camera and SZX7 scope, 30 min after the worms were transferred to 60 mm plates, for the duration of 1 min. ImageJ was used for processing: median filter followed by B/W thresholding and particle analysis to remove small dirt/precipitate particles. The processed videos were loaded into the δVision movement analysis software to determine the movement parameters (Delta Informatika Zrt, Hungary).

Chemotaxis and thermotaxis analysis

Chemotaxis assays were performed with synchronous adult animals at 20 °C as previously described [35]. Worms were washed three times with CTX buffer (1 mM $CaCl_2$, 1 mM $MgSO_4$, 5 mM KH_2PO_4 pH 6.0), and about 200 placed at the origin point of a 10-cm plate that was equidistant to the attractants, diacetyl (DA, 1% in absolute ethanol) or isoamyl alcohol (IA, 10% in absolute ethanol) and vehicle (absolute ethanol) point. NaN_3 (1 M) was added to the attractant and vehicle points of the plates, to prevent the worms from moving once they reach the attractants and vehicle. After 1 h worm's distribution over the plate was calculated and the chemotaxis index determined as previously described [35]. The thermotaxis paradigm was based on radial thermal gradients [48]. Radial thermal gradients were created by placing a 40-ml flask filled with 90% frozen acetic acid on top of an inverted 9 cm 10 ml NGM plate, in a room at 25 °C. The experimental setup was confirmed by time course analysis of agar temperatures with a thermometer with ± 0.4 °C accuracy. 15 min after the formation of the gradient a single worm was transferred to the 25 °C region of the plate with the use of an eyelash. After a period of 1 h the worm was removed and the tracks were outlined with a marker and imaged. Worms were classified according to the position of the tracks in the thermal gradient.

Lifespan and osmotic-, oxidative- and thermo-tolerance assays

For standard lifespan assays around 100 L4 animals, per strain, were placed in freshly seeded plates. Animals were kept at 20 °C and checked daily for viability. For tolerance assays, animals were subjected to distinct stresses and checked for viability every 2 in 2 h. For heat shock

Table 4 List of primers used for qRT-PCR

C. elegans gene	Forward primer	Reverse primer
SNX1/2	GACGCTAGTGGCTTCTCGTA	TCTCAGTGACGTCGGTCAGT
SNX3/12	GTGATTTCGAATGGGTTCGT	AGCGTTCGTTTTGAGCAAGT
SNX5/6	GAAGCCGAACAATCAGAAGC	AGAACTCTTGAGCCGTTCCA
SNX9	GCCTGACAGAAGCTCTCGC	ACAGTGTAGCTCATCGCATCG
SNX13/25	GCCGCTGAGATTCTTGCTT	GATGTTGAACTCGTGAGACAC
SNX17	CTCATTTCGTGCCACAAGCC	CACGTCCTTTTGCCATGAAC
SNX27	CATGTGAGTGCAGTGCTTCG	TGCCATTGAACTCTCTTCTCCA

experiments, synchronized young adult animals were grown at 20 °C and then transferred to 35 °C in a temperature controlled incubator and checked every 2 h for death. To perform pre-heat shock, animals were placed for 2 h at 30 °C and then transferred to 35 °C and checked every 2 h for death [36, 37]; for the osmotic stress, synchronous young adult animals were placed in freshly seeded plates with distinct NaCl concentrations (50, 200 and 400 mM) and checked every 4 h for dead animals [38]; for oxidative stress, synchronized young adult animals were placed in freshly seeded plates with distinct H_2O_2 concentrations (5, 10 and 20 mM) and checked every 4 h for dead animals [39]. More than 50 animals were analyzed per strain per experiment, and at least three independent replicates were performed for each assay.

Confocal imaging

For confocal imaging Δ*snx-s* mutants were crossed with the EG1285 and OH3701 marker strains. Around 10 L4 stage animals from the generated *C. elegans* lines were paralyzed in 1 M sodium azide and mounted on 3% agarose pads (diluted in M9 buffer). All images were captured on Olympus FV1000 (Japan) confocal microscope, under 60× oil objective. Multi-channel time-lapse images were acquired as Z-stacks (50 images) using epifluorescence mode with GFP filter cube. Images were compressed and assembled to generate a single image at each point on ImageJ. Complete documentation of each worm was performed via multi-area time-lapse acquisition. Individual images were assembled into a complete worm image using the ImageJ stitching plugin [40].

Statistical analysis

One-way ANOVA was used to analyze length measurements, motility, chemotaxis to DA and IA, SNXs expression levels throughout development. Bonferroni post-hoc test or Games-Howell (when equal variances were not assumed) was used to counteract the problem of multiple comparisons within each experiment. Student's *t* test was used to analyze the angle formed by the AIY neuronal processes. Non-parametric independent samples Mann–Whitney *U* test was used for crawling speed analysis. Animal survival (lifespan and stress assays) was plotted using Kaplan–Meier survival curves and analyzed by log rank test. Neuronal GABAergic defects were analyzed with Pearson Chi square test. A $p < 0.05$ was considered as statistically significant, and all tests were performed with the SPPS Statistics program (IBM SPSS Statistics, Armonk, NY, USA). A Bonferroni correction was applied to correct for possible false positive outcomes resulting from the large number of models (ANOVAs) applied.

Results

SNXs are phylogenetically conserved from *C. elegans* to mammals

An unrooted tree illustrating the phylogenetic relationship between the eight proposed SNXs orthologs encoded in the *C. elegans* genome and their predicted mammalian orthologs is represented on Fig. 1a. SNXs have been identified across phyla from mammals to yeasts [41] and are divided in three subfamilies according to the presence or absence of functional domains: those containing just a PX domain, those containing an additional C-terminal Bar (Bin-Amphiphysin-Rys) domain and those that contain other domains besides the PX domain, many of which are involved in cell signaling [1]. The close aminoacidic sequences relationship between *C. elegans* SNXs and the mammalian SNXs is illustrated on Fig. 1. More specifically: (1) SNX-1 clusters with mammalian SNX1/SNX2; (2) SNX-3 with mammalian SNX3/SNX12; (3) SNX-6 with mammalian SNX5/SNX6; (4) SNX-9/LST-4 with SNX9/SNX18; (5) SNX-13 resembles mammalian SNX13/SNX25; (6) SNX-14 is related to mammalian SXN14 but also to all SXN13/SNX25 orthologs; (7) SNX-17 clusters with mammalian SNX17 and (8) SNX-27 with mammalian SNX27. A domain conservation analysis was performed which confirmed an extremely high degree of identity and similarity between SNXs functional domains across phyla (Fig. 1b–d).

SNXs are differentially expressed during *C. elegans* developmental cycle

To get insights into the dynamics of SNXs expression in *C. elegans*, we performed qRT-PCR analysis using wild-type animals (N2) from different stages of development (from egg to adulthood) (Fig. 1e). Our results demonstrate that despite the sequence homology of the *C. elegans* SNXs members, their expression profile is distinct and dynamic over time (Fig. 1e). During the embryonic phase, SNXs expression differs significantly between each other [$F(6,7) = 166.42$, $p < 0.001$, $\eta^2 = 0.99$]. A post-hoc comparison indicates that the expression of: *snx-1* is distinct from *snx-5* and *snx-9*; *snx-3* is distinct from *snx-5*, *snx-13* and *snx-27*; *snx-5* is distinct from all tested SNXs; *snx-9* is distinct from *snx-1*, *snx-5*, *snx-13* and *snx-27*; *snx-13* is distinct from *snx*-3, *snx-5,* and *snx-9*; *snx-17* is distinct from *snx-5*; and *snx-27* is distinct from *snx-3*, *snx-5* and *snx-9*. During the L1.L2 phase, SNXs expression differs significantly between each other [$F(6,7) = 31.21$, $p < 0.001$, $\eta^2 = 0.96$]. A post-hoc comparison indicates

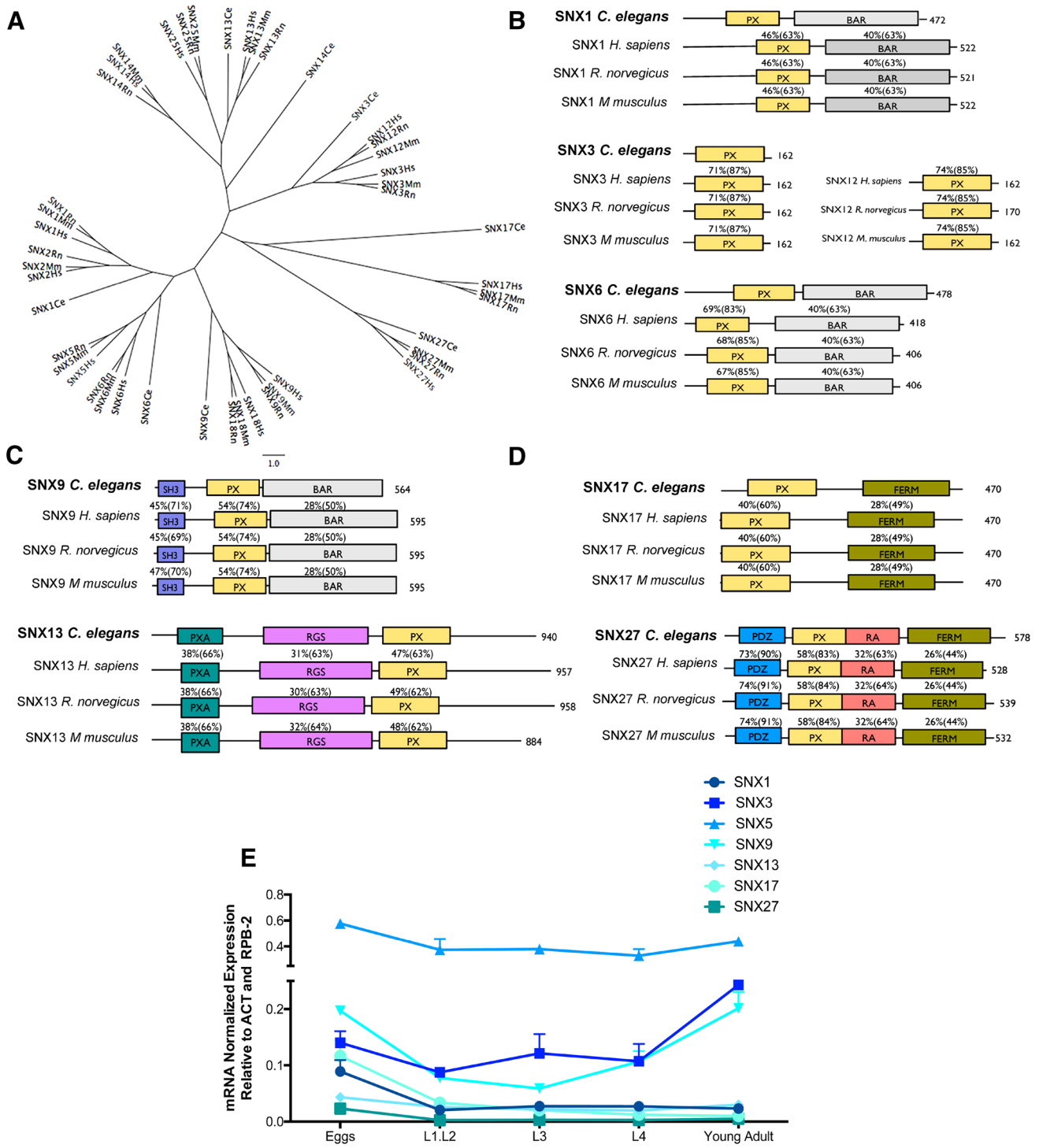

that *snx-5* expression is significantly different from all others. On the L3 phase SNXs expression also differs significantly between each other [$F(6,7) = 158.91$, $p < 0.001$, $\eta^2 = 0.99$]. Post-hoc analysis indicates that *snx-3* and *snx-5* are statistically different from all other SNXs. Regarding the L4 stage, SNXs expression is also distinct between each other [$F(6,7) = 46.88$, $p < 0.001$, $\eta^2 = 0.96$]. Post-hoc analysis indicates that only *snx-5* expression differs significantly from all other SNXs. Finally, on the adult phase SNXs expression also differs [$F(6,7) = 276.50$, $p < 0.001$, $\eta^2 = 0.99$], with the post-hoc analysis confirming that *snx-3*, *snx-5* and *snx-9* differ from all others, and with each other. In summary, *snx-5* is the SNX with the highest expression and its expression level is constant throughout

◂**Fig. 1** Phylogenetic analysis of SNXs orthologs and their developmental expression in *C. elegans*. **a** Unrooted tree representing the phylogenetic relationship between SNX orthologs. The corresponding aminoacidic sequences were analyzed using ClustalW for sequence alignment and PHYLIP for tree plotting. **b–d** Representation of *C. elegans* SNXs domain structure and their mammalian orthologs. The percentage of amino acid identity and (similarity) between *C. elegans* protein sequences and its mammalian homologs is also represented. *PX* phox homology, *BAR* Bin-amphiphysin-Rvs, *SH3* Src homology, *PXA* PX-associated domain, *RGS* regulators of G protein signaling, *FERM* F for 4.1 protein, E for ezrin, R for radixin and M for moesin, *PDZ* P for post-synaptic density protein (PSD95), D for drosophila disc large tumor suppressor (Dlg1), and Z for zonula occludens-1 protein (zo-1), *RA* Ras-association. **e** qRT-PCR expression analysis of distinct SNXs during development is represented in function of the developmental stage. SNXs are strongly expressed in the egg and adult stages and SNX5 is the most expressed SNX throughout *C. elegans* development. Independent experiments were performed with $n > 200$ per developmental stage. One-way ANOVA was performed and data represented are mean ± SD $^{*}p < 0.05$; $^{**}p < 0.01$; $^{***}p < 0.001$). Statistical analysis demonstrated that during the embryonic stage the expression of *snx-1* is distinct from *snx-5* and *snx-9* ($p < 0.00$; $p = 0.026$, respectively); *snx-3* expression is distinct from *snx-5*, *snx-13* and *snx-27* expression levels ($p < 0.000$, $p = 0.048$, $p = 0.16$, respectively); *snx-5* expression is distinct from all tested SNXs ($p < 0.000$); *snx-9* expression is distinct from *snx-1*, *snx-5*, *snx-13* and *snx-27* expression levels ($p = 0.026$, $p < 0.001$, $p = 0.003$ and $p = 0.001$ respectively); *snx-13* expression is distinct from *snx*-3, *snx-5* and *snx-9* expression levels ($p = 0.048$, $p < 0.001$, $p = 0.003$, respectively); *snx-17* expression is distinct from *snx-5* ($p < 0.000$); and *snx-27* expression is distinct from *snx-3*, *snx-5* and *snx-9* ($p = 0.016$, $p < 0.001$, $p = 0.001$, respectively). During the L1.L2 phase, SNXs expression differs significantly between each other [$F(6,7) = 31.21$ $p < 0.001$]. A post-hoc comparison indicates that *snx-5* expression is significantly different from all others ($p \leq 0.001$ for all). On the L3 phase SNXs expression also differs significantly between each other [$F(6,7) = 158.91$ $p < 0.001$]. Post-hoc analysis indicates that *snx-3* and *snx-5* expression levels are statistically different from all other SNXs (*snx-3*:$0.087 > p \leq 0.001$; *snx-5* $p \leq 0.001$ for all). Regarding the L4 stage, SNXs expression is also distinct between each other [$F(6,7) = 46.88$, $p < 0.001$]. Post-hoc analysis indicates that only *snx-5* expression differs significantly from all other SNXs ($p \leq 0.001$ for all). On the adult phase SNXs expression also differs [$F(6,7) = 276.50$, $p < 0.001$], with the post-hoc analysis confirming that *snx-3*, *snx-5*, and *snx*-9 differ from all others, and with each other ($p < 0.001$)

development, whereas *snx-1*, *snx-13*, *snx-1,7* and *snx-27* expression is generally lower and more evident during embryonic development (Fig. 1e). *Snx-3* and *snx-9* expression is higher than *snx-17* and *snx-27* expression throughout development, being more prominent during embryonic and adult stages (Fig. 1e).

Loss of *snx-3* expression leads to impaired worm development and reduced lifespan

To understand the impact of disrupted SNXs expression on *C. elegans*, a battery of developmental tests and morphological evaluation was applied. All the mutants were backcrossed eight times to wild-type animals, in order to eliminate additional mutations that could influence the phenotype [42]. Of the eight proposed SNXs orthologs in *C. elegans*, seven deletion mutants were viable and used in this study. All the selected Δ*snx-s* mutants presented large deletions and/or insertions in their coding regions, without interference with nearby genomic sequences.

To analyze the morphology of the Δ*snx-s* mutants during the *C. elegans* developmental cycle, we captured several images for automated analysis with the ImageJ/Fiji program. Overall, Δ*snx-s* mutants presented no evident morphological defects, with exception to the Δ*snx-3* mutant worm, which was smaller throughout development (Fig. 2a) [day 1: $F(7392) = 18.24$, $p < 0.001$, $\eta^2 = 0.25$; day 2: $F(7392) = 9.47$, $p < 0.001$, $\eta^2 = 0.15$; day 3: $F(7391) = 21.36$, $p < 0.001$, $\eta^2 = 0.28$; day 4: $F(7363) = 4.82$, $p < 0.001$, $\eta^2 = 0.09$], comparing to control (wild-type animals). Since equal variances were not present a post-hoc comparison using the Games-Howell test was performed, which demonstrated that similarly to the Δ*snx-3* mutant, Δ*snx-13* mutants were also significantly different from wild-type strain on day 1 ($p < 0.001$); and that on day 3 the length of Δ*snx-9* mutants was also significantly different from wild-type strain ($p < 0.001$; $p = 0.014$, respectively). Taking into consideration Δ*snx-3* mutant smaller body size, which implies impaired development, we also monitored Δ*snx-3* mutant *ex-utero* development from egg to adulthood and confirmed that Δ*snx-3* mutant displays a slower development rate when compared to wild-type worms (Fig. 2b). For instance, at 52 h after egg-laying about 95% of wild-type worms have reached the L4 stage, whereas only around 28% of Δ*snx-3* deletion mutant reached the L4 stage. Δ*snx-3* mutant also displayed a significantly reduced brood size, such as Δ*snx-5* mutant, when comparing to the wild-type strain [$F(7112) = 153.28$, $p < 0.001$, $\eta^2 = 0.90$]. Since equal variances were not observed a post-hoc comparison using the Games-Howell test was performed, which demonstrated that Δ*snx-3* and Δ*snx-5* mutants brood size are significantly different from the wild-type strain brood size (Δ*snx-3*: mean (M) = 47.1, standard deviation (SD) = 16.8; Δ*snx-5:* $M = 207.1$, SD = 34; N2: $M = 294.3$, SD = 17.8), $p < 0.001$ for both comparisons (Fig. 2c). All the other Δ*snx-s* deletion mutants showed normal progeny size. Finally, we assessed Δ*snx-3* lifespan, using as control wild-type worms, the short-lived mutant *daf-16* (*mu86*) and the long-lived *daf-2* (*e1370*) mutant [43–45]. Δ*snx-3* mutation significantly reduced *C. elegans* lifespan (Fig. 2d) ($p < 0.001$, Kaplan–Meier survival curves and log-rank analysis).

Loss of SNX-3 leads to neurobehavioral deficits

To investigate the potential role of s*nx-s* in the CNS we performed a battery of neurobehavioral tests. Regulation of motility is a complex biological process that relies on

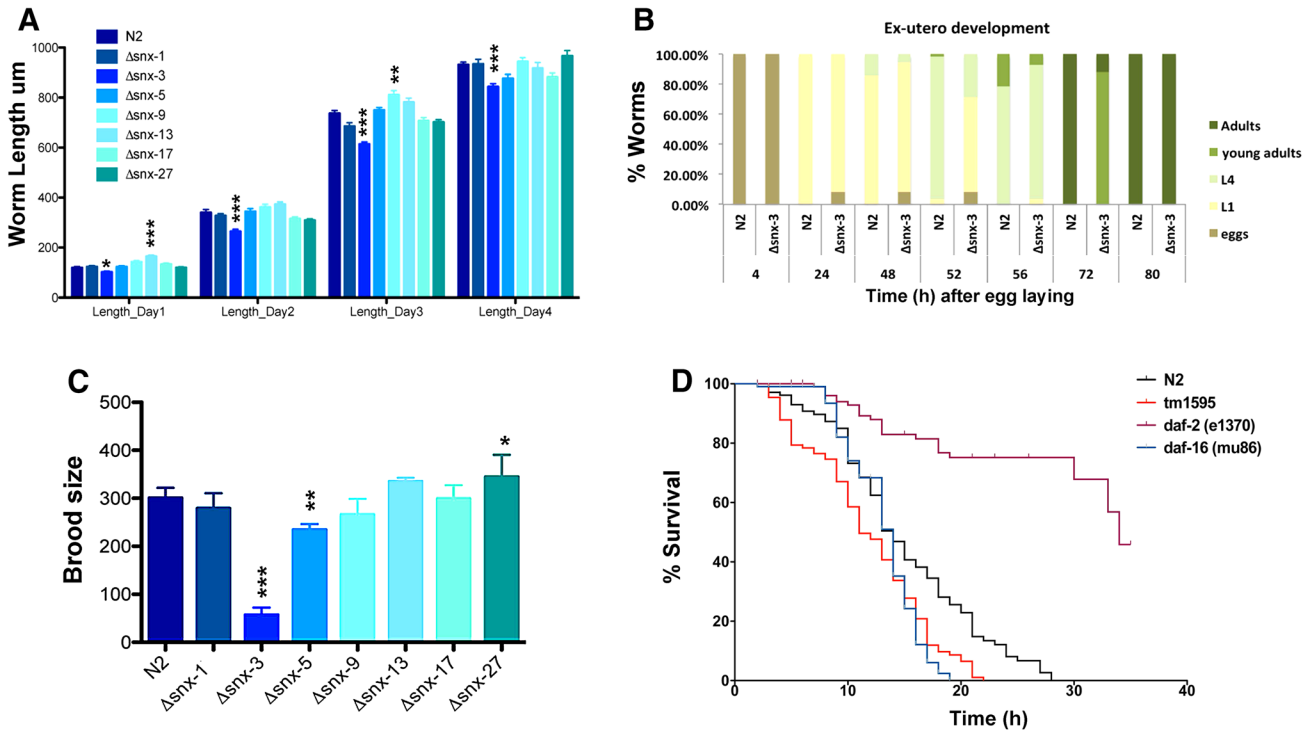

Fig. 2 Phenotypic analysis of SNXs deletion mutants. **a** Body length measurements of Δ*snx-s* mutants. The body lengths were measured 12, 36, 60 and 84 h after bleaching; 40–50 worms were studied per genotype, per day. It is noteworthy the significant smaller size of the Δ*snx-3* mutant throughout development, comparing to wild-type animals. One-way ANOVA analysis was performed and data represented as mean ± SEM. Error bars correspond to standard error $*p < 0.05$. **b** Time-course analysis of Δ*snx-3* mutant development. Animals were allowed to lay eggs and develop at standard conditions. Δ*snx-3* mutant has a delayed *ex-utero* development comparing to wild-type strain. **c** Brood size calculation of the distinct Δ*snx-s* mutants. Worm progeny at standard conditions was calculated per worm and per strain, on three independent assays. Δ*snx-3* mutant has a markedly reduced progeny size. Error bars correspond mean ± SD. **d** Lifespan analysis of the Δ*snx-3* mutant. Animals were grown at standard conditions and *daf-2*(*e1370*) and *daf-16*(*mu86*) used as controls. Δ*snx-3* mutant worms display a reduced survival comparative to wild-type worms ($p < 0.001$, Kaplan–Meier, log-rank analysis). Lifespan curve is representative of three independent experiments with $N > 100$, per experiment. Δ*snx-3* mutant survival is significantly distinct from the wild-type strain in all three experiments (p always < 0.001) $*p < 0.05$; $**p < 0.01$; $***p < 0.001$

the precise coordination between sensory, motor and contractile systems. Lack of coordination is often found in *C. elegans* mutants that present neuronal dysfunction [30]. Loss of *snx-3* resulted in significant reduction of motility when compared to age-matched wild-type worms [$F(9,27) = 9.85$, $p < 0.001$, $\eta^2 = 0.70$; post-hoc Bonferroni test: *snx-3* mutant $M = 46.9\%$ with SD = 6.1% comparing to $M = 19.13\%$ with a SD = 6.2% of the wild-type strain; $p < 0.001$] (Fig. 3a). Those locomotor impairments were not observed in other Δ*snx*-s mutants (Fig. 3a). To confirm Δ*snx-3* mutant motility defect, its crawling speed was quantified in the presence or absence of a food source (OP50) and in the presence or absence of external stimuli (tap) (Fig. 3b). Clearly, Δ*snx*-3 mutant worms are significantly slower than the wild-type worms, in all the tested conditions ($p < 0.05$ in the presence of a food source; $p < 0.001$ in starvation and in the presence of stimuli). Interestingly, both wild-type and Δ*snx-3* mutants respond by increasing their velocity in a similar manner (about 30 μm/s) when stimulated by tapping.

To assess the function of the sensory system in the Δ*snx*-3 mutant we quantified its chemotaxis behavior to two distinct volatile attractants: Isoamyl alcohol (IA) (Fig. 3c), and Diacetyl (DA) (Fig. 3d) that are dependent on the AWC and AWA sensory neurons, respectively [46]. Δ*snx-3* mutant showed an evident decrease in the chemotaxis index (CI) towards IA but not to DA (Fig. 3c, d) [$F(9,20) = 18.70$, $p < 0.001$, $\eta^2 = 0.89$; post-hoc Bonferroni test: Δ*snx-3* mutant—$M = 0.42$, SD = 0.08; wild-type—$M = 0.76$; SD = 0.05; $p < 0.001$], when compared to wild-type worms. This chemotaxis defect is not present in all the other tested Δ*snx-s* worms (Fig. 3c). To further explore the function of the sensory system in the Δ*snx*-3 mutant we monitored its thermotaxis behavior. Thermotaxis relies on thermosensory neurons that sense and memorize environmental temperature and in this manner regulate strategic behaviors in the worm [47]. Animals are able to remember their cultivation temperature and migrate towards, and move isothermally around it, on a spatial temperature gradient [48]. Clearly, Δ*snx-3*

mutant displays an impaired thermotaxis behavior, with deficits on isothermal tracking and on migration towards colder temperatures (cryophilic phenotype) (Fig. 3e).

Taking into consideration SNX-3 reported role in Wnt signaling and Wls recycling through the retromer complex [15], we quantified the locomotion impairments of a general retromer mutant (*vps-35*), of a Wnt signaling mutant (*egl-20*); and of two Wls mutants [*mig-14* (*ga62*) and *mig-14* (*mu71*)] that partially disrupt mig-14 function, and vary in their penetrance (*mu71* mutant is weaker) (Fig. 3f). Notably, the Wls *mig-14* (*ga62)* mutant displays a more pronounced motor impairment ($M = 59\%$, SD = 11.7%). Curiously, *mig-14* (*mu71*) mutant, that like *ga62* only partially disrupts *mig-14* function, has no obvious motor impairments ($M = 25.6\%$, SD = 1.2%). It should be noted that *mu71* is regarded as a weaker *mig-14* mutant. Regarding the Wnt signaling *egl-20* (*n585*) mutant and the general retromer mutant *vps-35* (*hu68*), both display marked locomotive defects, ($M = 46.5\%$, SD = 3.8% and $M = 48.5\%$, SD = 13.7%, respectively) (Fig. 3f). Chemotaxis index to IA of the above-mentioned retromer and Wnt mutants was also assessed. Remarkably, none of the Wnt signaling, Wls or retromer mutants displays impairments in their chemotaxis behavior towards IA (Fig. 3g), indicating that defective chemotaxis in the Δ*snx-3* worm is not retromer or Wnt-dependent. Thermosensation could not be monitored in the retromer and Wnt related mutants, as the mutant worms did not move on the thermal gradient (data not shown).

Taking into account all the described developmental and neurobehavioral deficits of the Δ*snx-3* worms, and the fact that those defects are not entirely present in the other *snx-s*, retromer and Wnt-related deletion mutants (genes considerably associated with the homeostasis of the nervous system), we decided to investigated possible compensatory mechanisms. For that purpose, we quantified the expression levels of the distinct *snx-s* by qRT-PCR in all the *snx-s*, retromer and wnt-related mutants (Fig. 3h). SNXs expression profile is quite stable in all the tested backgrounds [*snx-1*: $F(11,12) = 2.40$, $p = 0.074$, $\eta^2 = 0.68$; *snx-3*: $F(11,12) = 2.10$ $p = 0.109$, $\eta^2 = 0.66$; *snx-5*: $F(11,12) = 7.14$ $p = 0.001$, $\eta^2 = 0.87$; *snx-9*: $F(11,12) = 4.55$, $p = 0.007$, $\eta^2 = 0.81$; *snx-13*: $F(11,12) = 0.925$, $p = 0.548$, $\eta^2 = 0.46$; *snx-17*: $F(11,12) = 44.42$, $p < 0.001$, $\eta^2 = 0.98$; *snx-27*: $F(11,12) = 0.488$, $p = 0.877$, $\eta^2 = 0.31$]. qRT-PCR analysis confirmed that the absence of *snx-3* expression does not overall significantly change the levels of expression of all the tested *snx-s*, in the distinct backgrounds, while comparing to the wild-type strain (Fig. 3h).

Neuroanatomical changes in *snx-3* mutants

In *C. elegans*, temperature and IA are sensed by AFD and AWC neurons that project to several neurons, including to the AIY interneuron, that plays a key role in the thermotaxis and chemotaxis response. Taking into consideration the chemotaxis and thermotaxis defects of the Δ*snx-3* mutant we hypothesize that there could be anatomical alterations in the Δ*snx-3* AIY interneuron. To test this, we analyzed AIY neuronal architecture in the Δ*snx-3* mutant worm. For that purpose the Δ*snx-3* mutant was crossed with a AIY::GFP tagged strain (OH3701). Images from the AIY interneuron, at the L4 stage, revealed that depletion of SNX-3 leads to a reduction of the angle formed between both AIY neuronal processes (Fig. 4a, b). Quantification analysis (> 15 animals) confirmed this finding (Fig. 4b).

Taking into consideration Δ*snx-3* mutant locomotion defects, we also assessed the architecture of all its GABAergic neurons. Δ*snx-3* mutant strain was crossed with the EG1285 strain in which all the GABAergic neurons (26 neurons) express GFP. Δ*snx-3* mutant worms were shown to present a significantly higher degree of distinct neuroanatomical GABAergic defects in comparison to the wild-type (Fig. 4c, d; > 15 worms; Chi square test: missing, gap, short, extra, break, branched, bridged, handedness, guidance, missing body, punctate cord—$p < 0.001$; crossed and blob in commissure—$p = 0.001$; mis-localized body—$p = 0.046$).

Snx-3 deletion affects the response to different stressors

In addition to temperature sensing, the amphid sensory neurons are also involved in *C. elegans* responses to stress, many of which are common between worm and mammals [49, 50]. To investigate Δ*snx-3* mutant ability to cope with distinct stresses, wild-type and mutant worms were exposed to adverse conditions such as thermal stress (Fig. 5a), osmotic stress (Fig. 5b) and oxidative stresses: paraquat (Fig. 5c) and H_2O_2 (Fig. 5d).

Regarding the thermotolerance assays at 35 °C, *snx-3* mutants present a reduced life span of 12.7 h, SD = 0.26, comparing to wild-type worms that display a median lifespan of 14.7 h, SD = 0.36 (Kaplan–Meier, $p < 0.0001$; 14% reduction in Δ*snx-3* mutant survival) (Fig. 5a). Worms were also exposed to a stress-threshold temperature of 25 °C for 2 h and then subjected to 35 °C. In both cases, worms display enhanced survival at 35 °C when comparing to strains grown at 20 °C (data not shown), still the mutant strain presents a reduced survival of about 25% ($p < 0.0001$).

To monitor Δ*snx-3* mutant susceptibility to osmotic stress, we exposed wild-type and mutant worms to NGM plates supplemented with 400 mM of NaCl (Fig. 5b). The mutant worms display a significantly reduced life span with a median survival of 8.0 h, SD = 0.59, comparing to the 13.6 h, SD = 0.22, of the wild-type worms ($p < 0.0001$; a 41% reduction in Δ*snx-3* mutant survival). Interestingly, the worms that survived were able to adapt and generate

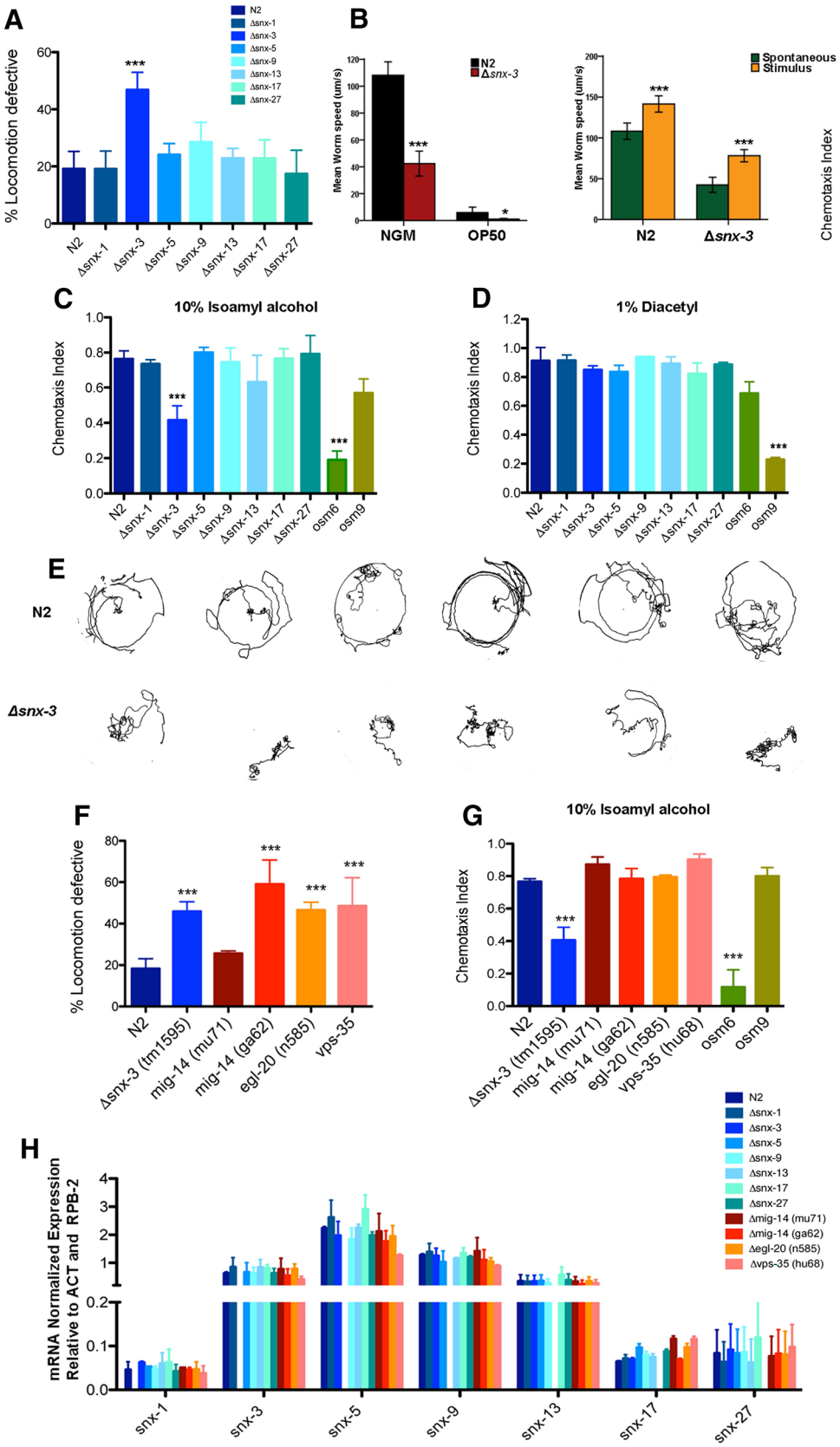
A
% Locomotion defective
N2
Δsnx-1
Δsnx-3
Δsnx-5
Δsnx-9
Δsnx-13
Δsnx-17
Δsnx-27
B
Mean Worm speed (um/s)
N2
Δsnx-3
NGM
OP50
Spontaneous
Stimulus
Chemotaxis Index
C
10% Isoamyl alcohol
Chemotaxis Index
osm6
osm9
D
1% Diacetyl
E
N2
Δsnx-3
F
% Locomotion defective
Δsnx-3 (tm1595)
mig-14 (mu71)
mig-14 (ga62)
egl-20 (n585)
vps-35
G
10% Isoamyl alcohol
Chemotaxis Index
vps-35 (hu68)
H
mRNA Normalized Expression
Relative to ACT and RPB-2
Δmig-14 (mu71)
Δmig-14 (ga62)
Δegl-20 (n585)
Δvps-35 (hu68)
snx-1
snx-3
snx-5
snx-9
snx-13
snx-17
snx-27

◂**Fig. 3** Behavioral characterization of SNXs deletion mutants. **a** Locomotion behavior of young adult worms (day 4, post-hatching) was analyzed for the indicated genotypes. Δ*snx-3* mutant displays increased motor impairments at standard growth conditions. Approximately 50% of the Δ*snx-3* mutant worms were unable to exit the 1 cm circle during the duration of the assay (60 s). Three independent experiments were performed with $N > 100$ per assay. One-way ANOVA analysis was performed and data represented as mean ± SEM; **b** average locomotion velocities were assessed in the presence/absence of a food source, such as OP50 or in the presence/absence of an external stimulus, such as tapping. Independent samples Mann–Whitney *U* test was performed. Disruption of *SNX-3* gene significantly affects worm's locomotive behavior, and reduces its crawling speed. **c**, **d** Chemotaxis index scores for SNXs mutants. Represented are the chemotaxis results of wild-type and SNXs mutant animals towards two volatile attractants (10% isoamyl alcohol, or 1% diacetyl). Chemotaxis index was calculated as CI (adults at the attractant minus the number of worms at the solvent, divided by the total number of worms in the plate [46]). Three independent experiments were performed with $N > 100$ per assay. One-way ANOVA analysis was performed and data represented as mean ± SD; **e** thermotaxis behavior of wild-type and Δ*snx-3* mutant in a temperature gradient. Δ*snx-3* mutant (second row) displays a cryophilic behavior, and is not able to perform isothermal tracking. **f** Locomotion behavior of young adult worms (day 4, post-hatching) was analyzed for the indicated genotypes. Δ*snx-3* mutant displays motor impairments at standard growth conditions, such as the stronger Wls (*mig-14*) mutant (ga62), the Wnt ligand mutant and the general retromer mutant. However, the weaker Wls (*mig-14*) mutant (mu71) presented no notorious locomotive defects, comparing to the wild-type strain. Approximately 46% of the *snx-3* mutant worms, 59% of *mig-14* mutant worms (stronger mutant), 47% of the *egl-20* mutant and 49% of the *vps-35* mutant worms were unable to exit the 1 cm circle during the duration of the assay (60 s). Three independent experiments were performed with $N > 100$ per assay. One-way ANOVA analysis was performed and data represented as mean ± SD. **g** Chemotaxis index scores for Wnt and retromer mutants. Represented are the chemotaxis results of wild-type and Wnt/retromer mutant animals towards a volatile attractants (10% isoamyl alcohol). Chemotaxis index was calculated as CI (adults at the attractant minus the number of worms at the solvent, divided by the total number of worms in the plate [46]). Clearly, Wnt signaling, Wls and retromer mutants display no deficits in its chemotaxis behavior towards IA, when compared to the wild-type strain (N2) or to *osm6* (perturbed chemotaxis to IA) and *osm9* (standard chemotaxis to IA) mutant controls. Data are the mean ± SD. ***$p < 0.001$. **h** qRT-PCR expression analysis of distinct *snx-s* in all the tested *snx-s*, retromer, and Wnt-related mutants. *Snx-s* are expressed in all the backgrounds, and *snx-5* is the most expressed *Snx*. It's noteworthy that *snx-3* expression is similar in wild-type and mutant strains, particularly in the retromer and Wnt-related mutants [$F(11,12) = 2.10$ $p = 0.109$]. Independent experiments were performed with $n > 200$ per mutant background. One-way ANOVA was performed and data represented are mean ± SD

progeny, but in the case of the Δ*snx-3* mutant worms the progeny was scarce and produced very few eggs, comparing to the wild-type after 24 h (data not shown).

In respect to oxidative stress (Fig. 5c, d), Δ*snx-3* mutant is more susceptible to: exposure to paraquat (10 and 20% reduction in Δ*snx-3* mutant survival in 100 and 200 mM, respectively; $p < 0.0001$); and to H_2O_2 (a reduction of approximately 25% in Δ*snx-3* mutant survival, in all tested conditions; $p < 0.001$). Median survival to paraquat exposure was of 11.5 h with a SD = 0.39 (100 mM) and 9.6 h, SD = 0.43 (200 mM), comparing to the median survival of 12.9 h, SD = 0.29 (100 mM) and 12.0 h, SD = 0.3 (200 mM) of the wild-type strain; median survival to H_2O_2 exposure was of 8.7 h, SD = 0.52 (5 mM H_2O_2); 7.8 h, SD = 0.54 (10 mM H_2O_2); 7.4 h, SD = 0.50 (20 mM H_2O_2); comparing to the 11.4 h, SD = 0.20 (5 mM H_2O_2); 10.9 h, SD = 0.36 (10 mM H_2O_2); 9.8 h, SD = 0.51 (20 mM H_2O_2) of the wild-type strain.

Re-expression of *C. elegans* snx-3 restores worm motor and chemotaxis behavior in snx-3 mutants

In order to investigate if the behavioral deficits of Δ*snx-3* mutant could be restored through the expression of *snx-3*, we generated constructs driving *C. elegans* or *H. sapiens snx-3* cDNA expression under the control of an ubiquitous (*eft-3p*) or pan-neuronal (aex-3p) promoters. Transgenic strains were generated by microinjecting the plasmids carrying the human or worm *snx-3* cDNAs (50 ng/µl), together with a marker plasmid which expressed mCherry under the control of the myo-2 promoter (5 ng/µl), as a transformation marker, into the wild-type background (N2).

Curiously, when *C. elegans snx-3* was expressed under the ubiquitous promoter *eft-3*, only one viable clone was obtained, which looked overall unhealthy and presented a very low plasmid transmission rate between generations (data not shown). No viable clones were obtained when *H. sapiens snx-3* was expressed under the same promoter (*eft-3p*), and only one clone was obtained when *H. sapiens snx-3* was expressed under the pan-neuronal (*aex-3p*) promoter, although also overall unhealthy and with a very low plasmid transmission rate between generations. This strongly suggests that worm and human *snx-3* cDNA expression levels must be finely regulated, since its ubiquitous "over"expression is detrimental for the worm survival. Moreover, it may indicate that worm and human expression/function may not be complementary, since the human protein is toxic to the worm.

In contrast, we were able to successfully obtain animals bearing the worm *snx-3* cDNA under the *aex-3* promoter, which were then crossed with the Δ*snx-3* mutant (*tm1595*)—*tm1595;SOUEx[paex-3::snx-3;pmyo::mcherry].*

Pan-neuronal expression of *snx-3* rescued Δ*snx-3* motor impairments and chemotaxis defects against isoamyl alcohol for all the tested lines (Fig. 6a, b). Specifically, *snx-3* pan-neuronal expression in the Δ*snx-3* worms improved motility of the worms when compared to age-matched wild-type worms [$F(5,27) = 13.59$, $p < 0.001$, $\eta^2 = 0.72$; post-hoc Bonferroni test: two independent lines displaying pan-neuronal *snx-3* expression: $M = 16.06\%$ with a SD = 6.29% ($p = 1$), and $M = 17.7\%$ with a SD = 6.95%; $p = 1$]. Two independent lines, with spontaneous loss of the

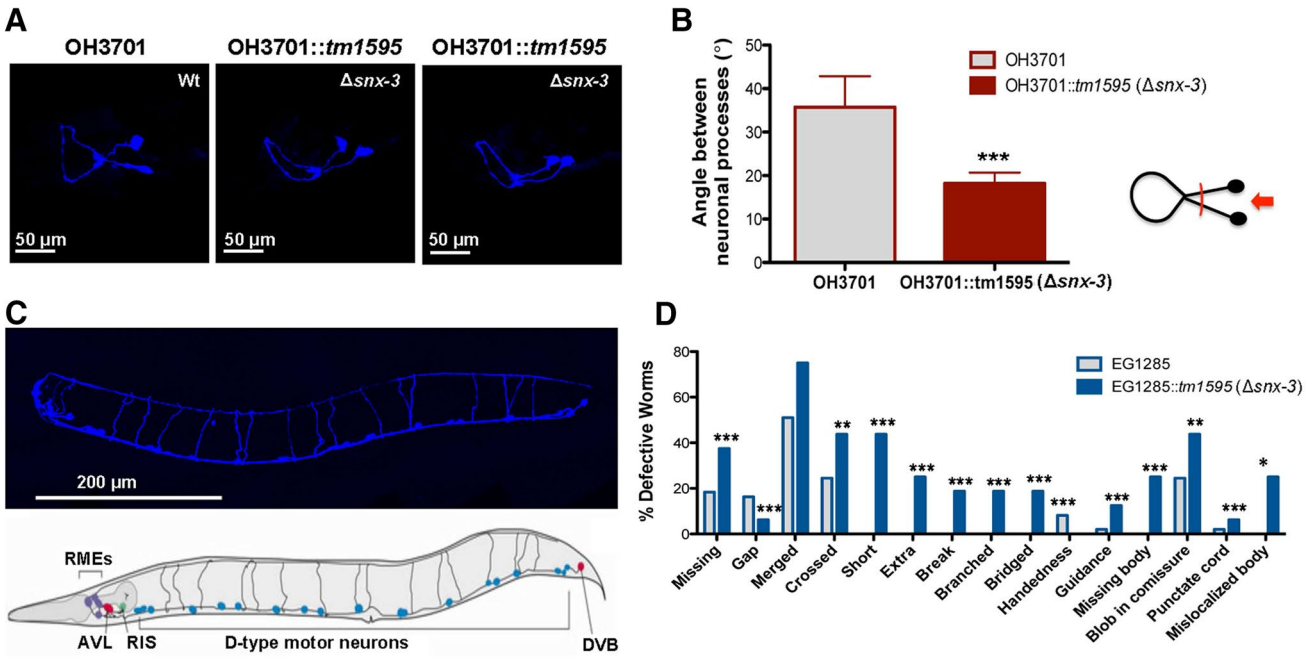

Fig. 4 Neuroanatomical analysis in the *Snx-3* mutant. **a** Structure of AIY interneuron in wild-type strain (OH3701) and in the Δ*snx-3* mutant strain (OH3701::*tm1595*). Representation of the maximal projections, of the 3D-reconstitutions, of the AIY neuronal structure (Wt, and two examples of the *snx-3* mutant). **b** Quantification of the angle formed by the neuronal processes of the AIY interneuron. Data was analyzed using Student's *t* test; mean ± SEM are represented. Clearly, both structures are distinct, namely, in what concerns the angle formed by its neuronal processes closer to the cell bodies, which is significantly smaller in the Δ*snx-3* mutant strain. **c** GABAergic neurons of Δ*snx-3* mutant (blue) comparing to the schematic representation of the GABAergic wild-type neurons. Depletion of *snx-3* impacts significantly on GABAergic neuronal wiring. **d** Quantification of GABAergic neuronal defects observed in > 15 animals per strain (Chi square test). *$p < 0.05$; **$p < 0.01$; ***$p < 0.001$

array, present, as expected, motility defects ($M = 34.80\%$ with a SD = 5.00% ($p = 0.017$); and $M = 38.53\%$ with a SD = 13.55% ($p = 0.02$) (Fig. 6a).

Pan-neuronal expression of *snx-3* in the Δ*snx-3* background also restored its ability to tract to IA, when compared to age-matched wild-type control [$F(5,18) = 16.33$, $p < 0.001$, $\eta^2 = 0.82$]; post-hoc Bonferroni test: two independent mutant clones displaying pan-neuronal *snx-3* expression: $M = 0.81$ with a SD = 0.09, $p = 1$; and $M = 0.83$ with a SD = 0.06, $p = 1$. The two lines that present spontaneous loss of the array, display deficits: $M = 0.58$ with a SD = 0.08, $p = 0.008$; and $M = 0.48$ with a SD = 0.10, $p < 0.001$ (Fig. 6b). This data shows that *snx-3* expression in neurons is sufficient to rescue Δ*snx-3* behavioral deficits.

Discussion

Caenorhabditis elegans SNXs are phylogenetically related to their mammalian counterparts

Distinct phylogenetic studies have demonstrated that SNXs are conserved across phyla and that higher eukaryotes display a wider array of PX domain proteins comparing to lower organisms. In fact, some of the PX domain subfamilies are not even present in lower organisms [2]. The mammalian genome encodes 34 predicted SNX proteins, comparing to the 8 predicted SNXs orthologs found in the *C. elegans* genome. In this work we have demonstrated that *C. elegans* SNXs orthologs are phylogenetically conserved between the *C. elegans* and mammals, that they are mostly from the PX-BAR domain subfamily, and that there is an evident domain conservation between its members, which implies functional conservation across phyla.

SNX-3 is essential for *C. elegans* development

Our findings regarding the *snx-3* deletion mutant clearly support a role for SNX-3 in worm development, since Δ*snx-3* mutant displays: (1) a small body size; (2) a delayed *ex-utero* development; (3) a reduced brood size; and (4) a shorter lifespan. Based on these evidences, and supported by the strong functional domain conservation between SNX family members, it is tempting to speculate that SNX-3 role in development can have important implications for related SNXs in the metazoan phylogeny. In *C. elegans*, such as in mammals, most SNXs belong to the PX-BAR domain containing subfamily, and 50% of them are involved with

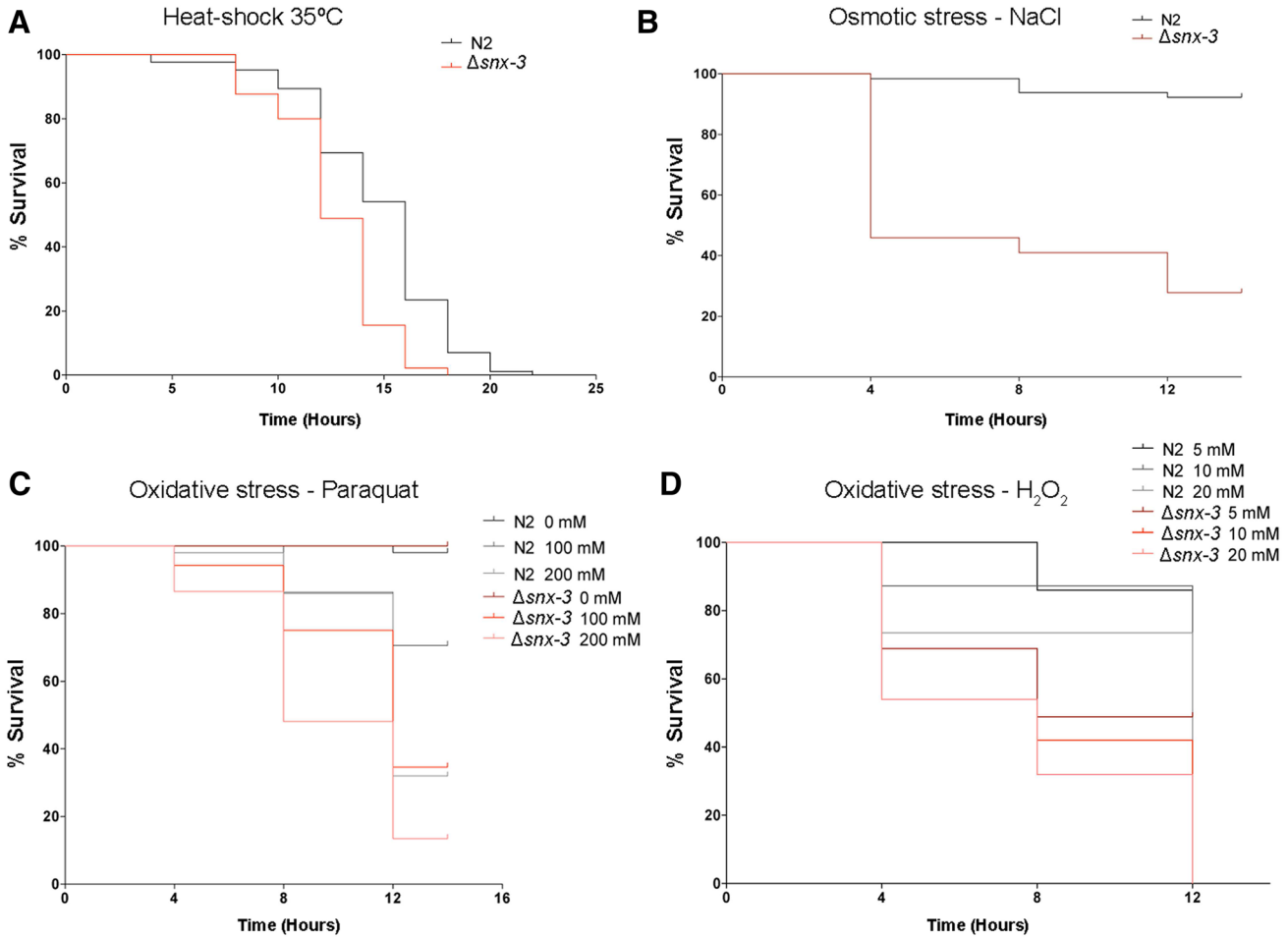

Fig. 5 *Snx-3* mutant susceptibility to stress. **a** Survival curve of wild-type (N2) and Δ*snx-3* young adults grown at 20 °C, upon a heat-shock at 35 °C. Δ*snx-3* mutant median survival is 12.7 h comparing to the wild-type survival of 14.7 h. **b** Survival curve of wild-type (N2) and Δ*snx-3* young adults exposed to an osmotic stress (NaCl 400 mM) for 12.0 h at 20 °C ($p < 0.001$). Δ*snx-3* mutant median survival is 8 h comparing to the wild-type survival of 13.6 h. **c**, **d** Survival curves of wild-type (N2) and Δ*snx-3* young adults exposed to distinct oxidative stress. **c** Synchronized young adults were exposed to different concentrations of Paraquat (100 and 200 mM) for 12 h. Δ*snx-3* mutant median survival is 11.5; 9.6 h (100 and 200 mM paraquat, respectively) comparing to the wild-type survival of 12.9; 12 h (100 and 200 mM paraquat, respectively). **d** Synchronized young adults were exposed to different concentrations of H_2O_2 (5, 10 and 20 mM) for 12 h ($p < 0.001$). Median survivals of Δ*snx-3* mutant: 8.7; 7.8; 7.4 h (5, 10 and 20 mM, respectively). Median survivals of N2: 11.4; 10.9; 9.8 h (5, 10 and 20 mM, respectively). For each survival assay, one representative experiment is presented from three independent replicates with similar results

cargo retrieval through the retromer complex. SNX3 is a PX-only domain containing protein that binds preferentially to PI(3)P [2]. Despite the literature controversy, it is recognized that SNX-3 plays a role in Wnt secretion (EGL-20), and in Wls (MIG-14) recycling through the retromer complex in *C. elegans*, *D. melanogaster* and in mammals [15], which could explain the Δ*snx-3* deletion mutant developmental defects. Accordingly, the available literature regarding Wnt mutants points to defects on cell division polarity, egg-laying, body length, erroneous neuronal migration, alterations in vulva morphology, among other defects (data from the Wormbase "https://www.wormbase.org/"), that imply impaired development. It has been demonstrated that SNX-3 directly interacts with the retromer components Vps-35 and Vps-26, that also co-immunoprecipitate with SNX-1 [15], to promote Wls (MIG-14) recycling. However, whether this is dependent or independent of other SNXs remains unclear [13, 23]. In fact, Shi and co-workers demonstrated that Δ*snx-1* mutants (*tm847*) display defective ALM posterior processes and defective PLM posterior processes, at a penetrance similar to the *vps-35* mutants (retromer component involved in Wls recycling and Wnt signaling), and missort Wls to the lysosome, similar to what has been shown in the Δ*snx-3* mutant (*tm1595*) [23]. Interestingly, distinct reports highlighted that in *C. elegans*, SNX-1 (a SNX1/SNX2 homolog) and SNX-3 (a SNX3/SNX12 homolog) regulate similar processes [51,

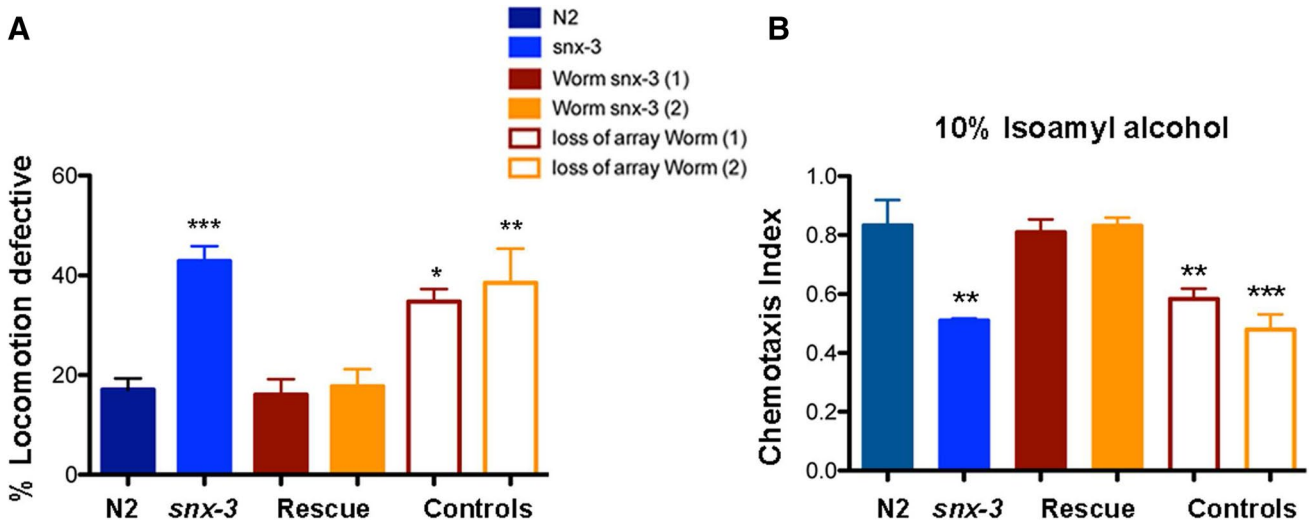

Fig. 6 Behavioral characterization of *C. elegans* Δ*snx*-3 strain with extrachromosomal expression of worm *snx-3* cDNA. **a** *C. elegans snx-3* expression rescues worm motility behavior of the Δ*snx-3* mutant. Locomotive behavior of two independent clones bearing pan-neuronal expression of *C. elegans snx-3* is represented, as well as of the worms with spontaneous loss of the array. Comparing to control (N2), and taking into consideration Δ*snx-3* mutant locomotive deficits, the mutant worms (1 and 2) with extrachromosomal expression of *snx-3* displayed a low percentage of locomotive deficits ($M = 16.06\%$ with a SD = 6.29% and $M = 17.7\%$ with a SD = 6.95%, $p = 1$ respectively); whereas the worms that spontaneously lose the array displayed deficits which resembled the Δ*snx-3* mutant ($M = 34.80\%$ with a SD = 5.00% and $M = 38.53\%$ with a SD = 13.55%, $p = 0.017$ and $p = 0.02$, respectively). Three independent experiments were performed with $N > 50$ per assay. One-way ANOVA analysis was performed and data represented as mean ± SD. **b** *C. elegans snx-3* expression rescues worm chemotraction to IA of the Δ*snx-3* mutant. Chemotaxis behavior of two independent clones bearing pan-neuronal expression of *C. elegans snx-3* is represented, as well as of the worms with spontaneous loss of the array. Comparing to control (N2), and taking into consideration Δ*snx-3* mutant chemotraction defects to IA, the mutant worms (1 and 2) with extrachromosomal expression of *snx-3* displayed higher CTX index ($M = 0.81$ with a SD = 0.09 and $M = 0.83$ with a SD = 0.06, $p = 1$ respectively); whereas the worms that spontaneously lose the array displayed a CTX index which resembled the Δ*snx-3* mutant ($M = 0.58$ with a SD = 0.08 and $M = 0.48$ with a SD = 0.10, $p > 0.001$, respectively). Three independent experiments were performed with $N > 200$ per assay. One-way ANOVA analysis was performed and data represented as mean ± SD

52], such as β-catenin localization [51] and amphid compartment morphogenesis, independently of other retromer components [52], implying overlapping functions. Oikonomou and co-workers used the same mutants employed in this study: Δ*snx-1* (*tm847*) and Δ*snx-3* (*tm1595*). Our findings indicate that disrupting SNX-3 (*tm1595*) alone leads to severe developmental defects that are not observed in other *C. elegans snx-s* mutants, that are known to partner with the retromer complex: Δ*snx-1* (*tm847*), Δ*snx-5* (*tm3790*) or Δ*snx-27* (*tm5356*). Specifically, no developmental defects were found in the Δ*snx-1* mutant, also purportedly involved in Wls recycling, with significant impact on the polarity of mechanosensory neurons [23]. Our results support the findings from Harterink and co-workers which refuted SNX-1 involvement in Wnt signaling, arguing that Δ*snx-1* mutant displays no QL.d positioning defects, that SNX-1 fails to co-immunoprecipitate with SNX-3 (that co-immunoprecipitates with the retromer complex), and that SNX-1 only partially co-localizes with SNX-3, suggesting the presence of two distinct retromer complexes [15]. However, we cannot discard the possibility that SNX-3 is involved in the recycling and/or degradation of other transmembrane cargoes that are important for worm development, that are not dependent on SNX-1. Namely, SNX-3 has been shown to regulate the correct sorting of the retrograde cargo type I TGF-β receptor (SMA-6) [24], whose mutation is associated with reduced body size [53]. Additionally, in mammals, SNX3 has been linked to endosomal morphology regulation [54] and intraluminal vesicle formation in multivesicular bodies (MVBs) aiding in this manner in cargo sorting to the degradative pathway, in a retromer-independent manner [55], and not only in cargo targeting to the trans-Golgi network (TGN); SNX-3 was also shown to regulate transferrin receptor recycling and iron assimilation, being highly expressed in vertebrate hematopoietic tissues [56].

Snx-3 ablation affects neuronal structure and worm behaviors

In the past decade, SNXs have been extensively linked to disease, particularly to brain pathology [2]. Several reports demonstrated the impact of SNXs expression dysregulation in the homeostasis of the CNS, namely in AD, DS, intellectual disability and in schizophrenia [3–10]. Particularly,

SNX3 has been associated with the homeostasis of the CNS in mammals, being linked to neurite outgrowth in vitro and its expression to be upregulated by lithium treatments [57]. Interestingly, SNX3 single-nucleotide polymorphisms (SNPs) have been found in AD patients [7]. An important role of SNX3 in the development of the nervous system is supported by its neuronal expression during development, and because some patients with microcephaly, microphthalmia, ectrodactyly, and prognathism (MMEP) and mental retardation present a disrupted SNX3 gene [58]. This could result from the SNX3 role on Wnt secretion, since there are several reports linking Wnt signaling and neuronal migration, differentiation, axon outgrowth and synaptic function, among others [59]. The effect of SNX3 on the CNS could also result from SNX3 interaction with other protein complexes, cytoskeletal proteins and regulatory adaptor proteins that promote neurite outgrowth, presently unknown. Our data clearly demonstrates for the first time in vivo, that SNX-3 is essential for the execution of specific worm behaviors. Δ*snx-3* mutants present severe impairments in its motor function, which are comparable to the locomotive defects of the tested Wnt and retromer mutants. Δ*snx-3* mutants also display a significantly reduced crawling speed in the presence or absence of external stimuli, although it is still able to trigger an increase in its velocity when facing an external stimulus such as tapping the plate. This could result from defects on neuronal structure and/or on synaptic transmission in motor neurons [60]. In fact, we show that Δ*snx-3* mutants display marked defects on their GABAergic neuronal structures, which are tightly involved with locomotion [61]. We have also demonstrated that Δ*snx-3* mutants present a reduced chemotaxis index towards the volatile attractant IA, which is sensed by AWC neurons, but displays no defects on its chemotaxis towards DA, which is sensed by AWA neurons. This could be due to the missorting of G-Protein-Coupled-Receptors in the absence of SNX-3, hence impairing the ability of *C. elegans* to sense one of the odors usually sensed by AWC neurons. It is noteworthy that G-Protein-Coupled-Receptors distribution is distinct between AWC and AWA neurons, and even between the pair of AWC neurons itself [46]. Remarkably, we have demonstrated that Δ*snx-3* mutant defects in chemotaxis behavior towards IA are independent of Wnt signaling and secretion, or general retromer function, since all of the above-mentioned mutants displayed standard chemotaxis index towards IA. This is a strong indication that, while the developmental deficits of Δ*snx*-3 may be explained by its role on Wls recycling and Wnt signaling, its impairments in chemotaxis, are independent of Wnt secretion, or retromer function. Moreover, this strengthens the notion that SNX-3 is involved in the recycling and/or degradation of other cargoes that are crucial for neuronal function, that are independent of its interaction with the retromer complex. Interestingly, AD and DS pathology have been associated with the dysregulation of distinct SNXs, being most of them involved with the retromer complex, whereas intellectual disability and schizophrenia have been associated with the dysregulation of SNXs belonging to the PXA-RGS-PX-PC SNX subfamily (SNX13, SNX14, SNX19 and SNX25), that are regulators of G-protein signaling (crucial for the worm chemotaxis behavior). It is relevant to highlight the role of SNX19 in the ethiopathogenesis of schizophrenia [9, 10], a disease with marked GABAergic dysfunction and neurodevelopmental impairments. It was demonstrated that elevated expression of SNX19 is associated with the risk of developing schizophrenia, as well as a SNP that in fact contributes to the disease [9, 11]. Curiously, the Δ*snx-3* mutant also presents "neuro"developmental defects and has impaired GABAergic neuronal wiring, which can suggest that there might be common molecular mechanisms altered in the absence of SNX3 and those found in schizophrenia. Altogether this supports a transversal role for SNXs spanning from neurodevelopmental processes to neurodegeneration with tremendous impact on the homeostasis of the nervous system. It remains to be elucidated, however, how SNX3 functions to maintain homeostasis of the nervous system, since not all of the worm observed behavioral defects are retromer- and Wnt-dependent. The chemotaxis defect could purportedly arise from an altered trafficking of GPCRs, in line with the above-mentioned role of the PXA-RGS subfamily. Interestingly, the absence of a RGS domain in the PX-only SNX3 does not impair this hypothesis, as SNX19 itself lacks this motif [62], and other SNXs that lack this domain have been reported to regulate GPCRs trafficking [63]. Moreover GPCRs heteromers have been shown to form in vitro with dopamine, serotonin, glutamate and adenosine receptors, whose trafficking regulation has been associated with SNXs [64].

Additionally, we have demonstrated that the Δ*snx-3* mutant also displayed a cryophilic behavior, implying a defect on the AFD sensory neuron, and/or in the interneurons, namely the AIY interneuron. Our findings show that the AIY interneuron displays an aberrant structure in the Δ*snx-3* mutant, what could explain its defective ability to chemotract to IA, and to perform isothermal tracking, an indirect measure of its sensory perception. Curiously, *C. elegans* SNX-3 has been associated with amphid sensory compartment size regulation, namely to promote sensory compartment growth in a manner similar to SNX-1 and VPS-29, which could explain why the angle formed by the AIY interneurons processes is narrower in the Δ*snx-3* mutant [52]. Interestingly, Oikonomou and co-workers demonstrated that Wnt signaling pathway is not involved in amphid sensory compartment formation and hence that SNX-3 acts on amphid morphogenesis most probably in a Wnt-independent manner [52], similar to what we have demonstrated above regarding chemotaxis behavior towards

IA in the Δ*snx-3*. Additionally, we observed no significant changes on *snx-3* expression levels on retromer, or Wnt-related mutants, comparing to the wild-type background, indicating the absence of compensatory mechanisms that could mask the observed behavioral phenotypes. Concomitantly, we clearly demonstrate that the worm motor and chemotaxis defects are due to the absence of SNX-3, since we were able to rescue these behavioral phenotypes when the worm *snx-3* cDNA was expressed in the Δ*snx-3* mutant background. Interestingly, rescue was observed when the cDNA was expressed under a pan-neuronal promoter, suggesting that *snx-3* expression in neurons alone was sufficient to restore the worm behavior. The human *snx-3* cDNA, although significantly conserved with the worm sequence, was toxic when expressed under the same promoters. This suggests that factors other than the level of sequence identity are important to determine if human genes can functionally complement in *C. elegans*. Possibly, and taking into consideration that the levels of *C. elegans snx-3* must be tightly regulated, as loss of *snx-3* leads to reduced-life span whereas high levels to lethality, expression regulation of the worm and human *snx-3* sequences under the tested conditions, are most likely not interchangeable.

Finally, we observed that SNX-3 is crucial for the worms' ability to "cope" and "adapt" to harmful situations. It is noteworthy that stress resistance and longevity are interrelated, since several pathways that regulate stress also regulate longevity, such as mitochondrial respiration, insulin/IGF-1 and JNK (c-Jun N-terminal kinase) signaling [65]. Usually, manipulations that reduce resistance to acute stressors also reduce longevity, suggesting that the ability to sense and respond to environmental cues is crucial for lifespan regulation, although sometimes with exceptions [65]. Our data clearly demonstrate that the short-lived Δ*snx-3* mutant has a decreased stress resistance, which may be linked to the reduced size of the amphid sensory compartment [52], and/or as we demonstrated in this work, to impairments in its sensory neurons, such as the AWC, or to impairments in communication through its interneurons, namely through the AIY neurons that are abnormal in the Δ*snx-3* mutant.

In summary, this study provides the first in vivo characterization of *C. elegans* SNXs mutant family, providing insights into the functional role of SNXs in *C. elegans*. Namely, of SNX-3 involvement in *C. elegans* neuronal development and behavior. Among the phylogenetically conserved and ubiquitously expressed SNX family members, *C. elegans snx-3* ablation was the only one that resulted in evident developmental and behavioral deficits that most probably result from abnormal neuronal structure, and hence function. Nonetheless, despite the vast phenotypical analysis performed in the scope of this work, one cannot discard the fact that distinct molecular pathways and/or behaviors, that were not tested, can be perturbed in those mutants. Additionally, the overexpression of SNXs could also be studied, since their up-regulation has also been reported to occur in pathology [66], and hence to impact on human health. Overall, our findings regarding SNXs ablation support the prominent role of SNX-3 in the regulation of the worm development and of its neuronal function. Moreover, we have demonstrated that SNX-3 role on worm chemotaxis behavior is independent of Wnt or general retromer function. The behavioral deficits and neuroanatomical changes present in the Δ*snx-3* mutant allow us to anticipate possible SNX3 roles in the nervous system of higher organisms, which needs to be further explored.

Acknowledgements This work has been funded by FEDER funds, through the Competitiveness Factors Operational Programme (COMPETE), and by National funds, through the Foundation for Science and Technology (FCT), under the scope of the Project POCI-01-0145-FEDER-007038; and by a 2016 NARSAD Young Investigator Grant (#24929) from the Brain and Behavior Research Foundation. This work was developed under the scope of the Project NORTE-01-0145-FEDER-000013, supported by the Northern Portugal Regional Operational Programme (NORTE 2020), under the Portugal 2020 Partnership Agreement, through the European Regional Development Fund (FEDER). NV is supported by the FCT Fellowship SFRH/BPD/91250/2012. AJR is an FCT Investigator IF/00883/2013. CB is supported by a FCT Grant SFRH/BPD/74452/2010 (POPH/FS). PM is supported by a fellowship from the project "Envelhecimento cognitivo saudável–proporcionar saúde mental no processo biológico do envelhecimento" (Contract P-139977) funded by Calouste Gulbenkian–Inovar em Saúde. Research in AXC's lab is funded by the European Research Council under the European Union's Horizon 2020 research and innovation programme (Grant agreement 640553-ACTOMYO). AXC has a FCT Investigator position funded by FCT and co-funded by the European Social Fund through Programa Operacional Temático Potencial Type 4.2 promotion of scientific employment. FC is supported by the FCT fellowship SFRH/BPD/93528/2013. We would like to thank all the members of the NeRD research domain, ICVS, for fruitful discussion and advices.

Compliance with ethical standards

Conflict of interest The authors declare that they have no conflict of interest.

References

1. Cullen PJ (2008) Endosomal sorting and signalling: an emerging role for sorting nexins. Nat Rev Mol Cell Biol 9:574–582
2. Teasdale RD, Collins BM (2012) Insights into the PX (phox-homology) domain and SNX (sorting nexin) protein families: structures, functions and roles in disease. Biochem J 441:39–59
3. Thomas AC, Williams H, Seto-Salvia N, Bacchelli C, Jenkins D, O'Sullivan M, Mengrelis K, Ishida M, Ocaka L, Chanudet E, James C, Lescai F, Anderson G, Morrogh D, Ryten M, Duncan AJ, Pai YJ, Saraiva JM, Ramos F, Farren B, Saunders D, Vernay B, Gissen P, Straatmaan-Iwanowska A, Baas F, Wood NW, Hersheson J, Houlden H, Hurst J, Scott R, Bitner-Glindzicz M, Moore GE, Sousa SB, Stanier P (2014) Mutations in SNX14 cause a distinctive autosomal-recessive cerebellar ataxia and intellectual disability syndrome. Am J Hum Genet 95:611–621

4. Zhao Y, Wang Y, Yang J, Wang X, Zhao Y, Zhang X, Zhang YW (2012) Sorting nexin 12 interacts with BACE1 and regulates BACE1-mediated APP processing. Mol Neurodegener 7:30
5. Lee J, Retamal C, Cuitino L, Caruano-Yzermans A, Shin JE, van Kerkhof P, Marzolo MP, Bu G (2008) Adaptor protein sorting nexin 17 regulates amyloid precursor protein trafficking and processing in the early endosomes. J Biol Chem 283:11501–11508
6. Schobel S, Neumann S, Hertweck M, Dislich B, Kuhn PH, Kremmer E, Seed B, Baumeister R, Haass C, Lichtenthaler SF (2008) A novel sorting nexin modulates endocytic trafficking and alpha-secretase cleavage of the amyloid precursor protein. J Biol Chem 283:14257–14268
7. Vardarajan BN, Bruesegem SY, Harbour ME, Inzelberg R, Friedland R, St George-Hyslop P, Seaman MN, Farrer LA (2012) Identification of Alzheimer disease-associated variants in genes that regulate retromer function. Neurobiol Aging 33:2231 e15–2231 e30
8. Wang X, Zhao Y, Zhang X, Badie H, Zhou Y, Mu Y, Loo LS, Cai L, Thompson RC, Yang B, Chen Y, Johnson PF, Wu C, Bu G, Mobley WC, Zhang D, Gage FH, Ranscht B, Zhang YW, Lipton SA, Hong W, Xu H (2013) Loss of sorting nexin 27 contributes to excitatory synaptic dysfunction by modulating glutamate receptor recycling in Down's syndrome. Nat Med 19:473–480
9. Zhu Z, Zhang F, Hu H, Bakshi A, Robinson MR, Powell JE, Montgomery GW, Goddard ME, Wray NR, Visscher PM, Yang J (2016) Integration of summary data from GWAS and eQTL studies predicts complex trait gene targets. Nat Genet 48:481–487
10. Hauberg ME, Zhang W, Giambartolomei C, Franzen O, Morris DL, Vyse TJ, Ruusalepp A, CommonMind C, Sklar P, Schadt EE, Bjorkegren JLM, Roussos P (2017) Large-scale identification of common trait and disease variants affecting gene expression. Am J Hum Genet 101:157
11. Fullard JF, Giambartolomei C, Hauberg ME, Xu K, Voloudakis G, Shao Z, Bare C, Dudley JT, Mattheisen M, Robakis NK, Haroutunian V, Roussos P (2017) Open chromatin profiling of human postmortem brain infers functional roles for non-coding schizophrenia loci. Hum Mol Genet 26:1942–1951
12. Bessa C, Maciel P, Rodrigues AJ (2013) Using *C. elegans* to decipher the cellular and molecular mechanisms underlying neurodevelopmental disorders. Mol Neurobiol 48:465–489
13. Sato K, Norris A, Sato M, Grant BD (2014) C. elegans as a model for membrane traffic. WormBook 1–47. https://doi.org/10.1895/wormbook.1.77.2
14. Seaman MN (2012) The retromer complex - endosomal protein recycling and beyond. J Cell Sci 125:4693–4702
15. Harterink M, Port F, Lorenowicz MJ, McGough IJ, Silhankova M, Betist MC, van Weering JR, van Heesbeen RG, Middelkoop TC, Basler K, Cullen PJ, Korswagen HC (2011) A SNX3-dependent retromer pathway mediates retrograde transport of the Wnt sorting receptor Wntless and is required for Wnt secretion. Nat Cell Biol 13:914–923
16. Loo LS, Tang N, Al-Haddawi M, Dawe GS, Hong W (2014) A role for sorting nexin 27 in AMPA receptor trafficking. Nat Commun 5:3176
17. Mecozzi VJ, Berman DE, Simoes S, Vetanovetz C, Awal MR, Patel VM, Schneider RT, Petsko GA, Ringe D, Small SA (2014) Pharmacological chaperones stabilize retromer to limit APP processing. Nat Chem Biol 10:443–449
18. Li C, Shah SZ, Zhao D, Yang L (2016) Role of the retromer complex in neurodegenerative diseases. Front Aging Neurosci 8:42
19. Verges M (2007) Retromer and sorting nexins in development. Front Biosci 12:3825–3851
20. Dang H, Klokk TI, Schaheen B, McLaughlin BM, Thomas AJ, Durns TA, Bitler BG, Sandvig K, Fares H (2011) Derlin-dependent retrograde transport from endosomes to the Golgi apparatus. Traffic 12:1417–1431
21. Worby CA, Dixon JE (2002) Sorting out the cellular functions of sorting nexins. Nat Rev Mol Cell Biol 3:919–931
22. Zhang Y, Grant B, Hirsh D (2001) RME-8, a conserved J-domain protein, is required for endocytosis in *Caenorhabditis elegans*. Mol Biol Cell 12:2011–2021
23. Shi A, Sun L, Banerjee R, Tobin M, Zhang Y, Grant BD (2009) Regulation of endosomal clathrin and retromer-mediated endosome to Golgi retrograde transport by the J-domain protein RME-8. EMBO J 28:3290–3302
24. Gleason RJ, Akintobi AM, Grant BD, Padgett RW (2014) BMP signaling requires retromer-dependent recycling of the type I receptor. Proc Natl Acad Sci USA 111:2578–2583
25. Bai Z, Grant BD (2015) A TOCA/CDC-42/PAR/WAVE functional module required for retrograde endocytic recycling. Proc Natl Acad Sci USA 112:E1443–E1452
26. van Weering JR, Verkade P, Cullen PJ (2010) SNX–BAR proteins in phosphoinositide-mediated, tubular-based endosomal sorting. Semin Cell Dev Biol 21:371–380
27. Lu N, Shen Q, Mahoney TR, Liu X, Zhou Z (2011) Three sorting nexins drive the degradation of apoptotic cells in response to PtdIns(3)P signaling. Mol Biol Cell 22:354–374
28. Popoff V, Mardones GA, Bai SK, Chambon V, Tenza D, Burgos PV, Shi A, Benaroch P, Urbe S, Lamaze C, Grant BD, Raposo G, Johannes L (2009) Analysis of articulation between clathrin and retromer in retrograde sorting on early endosomes. Traffic 10:1868–1880
29. McGough IJ, Cullen PJ (2013) Clathrin is not required for SNX-BAR-retromer-mediated carrier formation. J Cell Sci 126:45–52
30. Brenner S (1974) The genetics of *Caenorhabditis elegans*. Genetics 77:71–94
31. Kuroyanagi H, Ohno G, Sakane H, Maruoka H, Hagiwara M (2010) Visualization and genetic analysis of alternative splicing regulation in vivo using fluorescence reporters in transgenic *Caenorhabditis elegans*. Nat Protoc 5:1495–1517
32. Edgar RC (2004) MUSCLE: a multiple sequence alignment method with reduced time and space complexity. BMC Bioinform 5:113
33. Pfaffl MW (2001) A new mathematical model for relative quantification in real-time RT-PCR. Nucleic Acids Res 29:e45
34. Zhang Y, Chen D, Smith MA, Zhang B, Pan X (2012) Selection of reliable reference genes in *Caenorhabditis elegans* for analysis of nanotoxicity. PLoS One 7:e31849
35. Bargmann CI, Hartwieg E, Horvitz HR (1993) Odorant-selective genes and neurons mediate olfaction in *C. elegans*. Cell 74:515–527
36. Prahlad V, Cornelius T, Morimoto RI (2008) Regulation of the cellular heat shock response in *Caenorhabditis elegans* by thermosensory neurons. Science 320:811–814
37. Rodrigues AJ, Neves-Carvalho A, Teixeira-Castro A, Rokka A, Corthals G, Logarinho E, Maciel P (2011) Absence of ataxin-3 leads to enhanced stress response in *C. elegans*. PLoS One 6:e18512
38. Lamitina ST, Morrison R, Moeckel GW, Strange K (2004) Adaptation of the nematode *Caenorhabditis elegans* to extreme osmotic stress. Am J Physiol Cell Physiol 286:C785–C791
39. Vertino A, Ayyadevara S, Thaden JJ, Shmookler Reis RJ (2011) A narrow quantitative trait locus in *C. elegans* coordinately affects longevity, thermotolerance, and resistance to paraquat. Front Genet 2:63
40. Preibisch S, Saalfeld S, Tomancak P (2009) Globally optimal stitching of tiled 3D microscopic image acquisitions. Bioinformatics 25:1463–1465
41. Carlton J, Bujny M, Rutherford A, Cullen P (2005) Sorting nexins—unifying trends and new perspectives. Traffic 6:75–82

42. Zuryn S, Le Gras S, Jamet K, Jarriault S (2010) A strategy for direct mapping and identification of mutations by whole-genome sequencing. Genetics 186:427–430
43. Wadsworth WG, Riddle DL (1989) Developmental regulation of energy metabolism in *Caenorhabditis elegans*. Dev Biol 132:167–173
44. Kenyon C, Chang J, Gensch E, Rudner A, Tabtiang R (1993) A *C. elegans* mutant that lives twice as long as wild type. Nature 366:461–464
45. Lin K, Dorman JB, Rodan A, Kenyon C (1997) daf-16: an HNF-3/forkhead family member that can function to double the life-span of *Caenorhabditis elegans*. Science 278:1319–1322
46. Wes PD, Bargmann CI (2001) *C. elegans* odour discrimination requires asymmetric diversity in olfactory neurons. Nature 410:698–701
47. Kimata T, Sasakura H, Ohnishi N, Nishio N, Mori I (2012) Thermotaxis of *C. elegans* as a model for temperature perception, neural information processing and neural plasticity. Worm 1:31–41
48. Hedgecock EM, Russell RL (1975) Normal and mutant thermotaxis in the nematode *Caenorhabditis elegans*. Proc Natl Acad Sci USA 72:4061–4065
49. Lant B, Storey KB (2010) An overview of stress response and hypometabolic strategies in *Caenorhabditis elegans*: conserved and contrasting signals with the mammalian system. Int J Biol Sci 6:9–50
50. Rodriguez M, Snoek LB, De Bono M, Kammenga JE (2013) Worms under stress: *C. elegans* stress response and its relevance to complex human disease and aging. Trends Genet 29:367–374
51. Kanamori T, Inoue T, Sakamoto T, Gengyo-Ando K, Tsujimoto M, Mitani S, Sawa H, Aoki J, Arai H (2008) Beta-catenin asymmetry is regulated by PLA1 and retrograde traffic in *C. elegans* stem cell divisions. EMBO J 27:1647–1657
52. Oikonomou G, Perens EA, Lu Y, Shaham S (2012) Some, but not all, retromer components promote morphogenesis of *C. elegans* sensory compartments. Dev Biol 362:42–49
53. Krishna S, Maduzia LL, Padgett RW (1999) Specificity of TGF-beta signaling is conferred by distinct type I receptors and their associated SMAD proteins in *Caenorhabditis elegans*. Development 126:251–260
54. Xu Y, Hortsman H, Seet L, Wong SH, Hong W (2001) SNX3 regulates endosomal function through its PX-domain-mediated interaction with PtdIns(3)P. Nat Cell Biol 3:658–666
55. Pons V, Luyet PP, Morel E, Abrami L, van der Goot FG, Parton RG, Gruenberg J (2008) Hrs and SNX3 functions in sorting and membrane invagination within multivesicular bodies. PLoS Biol 6:e214
56. Chen C, Garcia-Santos D, Ishikawa Y, Seguin A, Li L, Fegan KH, Hildick-Smith GJ, Shah DI, Cooney JD, Chen W, King MJ, Yien YY, Schultz IJ, Anderson H, Dalton AJ, Freedman ML, Kingsley PD, Palis J, Hattangadi SM, Lodish HF, Ward DM, Kaplan J, Maeda T, Ponka P, Paw BH (2013) Snx3 regulates recycling of the transferrin receptor and iron assimilation. Cell Metab 17:343–352
57. Mizutani R, Yamauchi J, Kusakawa S, Nakamura K, Sanbe A, Torii T, Miyamoto Y, Tanoue A (2009) Sorting nexin 3, a protein upregulated by lithium, contains a novel phosphatidylinositol-binding sequence and mediates neurite outgrowth in N1E-115 cells. Cell Signal 21:1586–1594
58. Mizutani R, Nakamura K, Yokoyama S, Sanbe A, Kusakawa S, Miyamoto Y, Torii T, Asahara H, Okado H, Yamauchi J, Tanoue A (2011) Developmental expression of sorting nexin 3 in the mouse central nervous system. Gene Expr Patterns 11:33–40
59. Rosso SB, Inestrosa NC (2013) WNT signaling in neuronal maturation and synaptogenesis. Front Cell Neurosci 7:103
60. Chalfie M, Sulston JE, White JG, Southgate E, Thomson JN, Brenner S (1985) The neural circuit for touch sensitivity in *Caenorhabditis elegans*. J Neurosci 5:956–964
61. Schuske K, Beg AA, Jorgensen EM (2004) The GABA nervous system in *C. elegans*. Trends Neurosci 27:407–414
62. Mas C, Norwood SJ, Bugarcic A, Kinna G, Leneva N, Kovtun O, Ghai R, Ona Yanez LE, Davis JL, Teasdale RD, Collins BM (2014) Structural basis for different phosphoinositide specificities of the PX domains of sorting nexins regulating G-protein signaling. J Biol Chem 289:28554–28568
63. Wang Y, Zhou Y, Szabo K, Haft CR, Trejo J (2002) Down-regulation of protease-activated receptor-1 is regulated by sorting nexin 1. Mol Biol Cell 13:1965–1976
64. Moreno JL, Holloway T, Gonzalez-Maeso J (2013) G protein-coupled receptor heterocomplexes in neuropsychiatric disorders. Prog Mol Biol Transl Sci 117:187–205
65. Zhou KI, Pincus Z, Slack FJ (2011) Longevity and stress in *Caenorhabditis elegans*. Aging (Albany NY) 3:733–753
66. Hao X, Wang Y, Ren F, Zhu S, Ren Y, Jia B, Li YP, Shi Y, Chang Z (2011) SNX25 regulates TGF-beta signaling by enhancing the receptor degradation. Cell Signal 23:935–946